ESTIMATION OF THE LEVEL OF QUASI-STATIC MICROACCELERATIONS ON BOARD OF THE SPACECRAFT IN ORBITAL ORIENTATION MODE

© 2025 A.I. Ignatov *
Bauman Moscow Technical State University, Moscow, Russia

**e-mail: general_z@mail.ru*

Received February 01, 2024
Revised February 24, 2024
Accepted March 07, 2024

The paper considers various options for implementing the orbital orientation mode of a spacecraft intended for conducting experiments in microgravity conditions over long time intervals. The system of gyroscopic controls (gyrosystem) is used as the actuators of the angular motion control system. The gyrosystem control laws proposed in the paper allow not only to provide a given orientation of the spacecraft, but also to limit the accumulation of the gyrosystem's own angular momentum, which significantly increases the duration of time intervals of unperturbed motion of the spacecraft. The efficiency of the considered control laws in the presence of external destabilizing disturbing moments acting on the spacecraft is confirmed by the results of numerical modeling of the equations of motion. The main orientation mode of the spacecraft investigated in the paper is its orbital orientation using gyrodamping. For this mode, an assessment of the level of quasi-static microaccelerations occurring on board the spacecraft is carried out, and the results of their spectral analysis are shown.

DOI: 10.31857/S00234206250110e1

INTRODUCTION

This work is devoted to the calculation of the level of microaccelerations occurring on board a spacecraft (SC) in its orbital orientation mode, as well as the analysis of their spectral characteristics. The SC under consideration is intended for conducting research in the field of microgravity over long time intervals. Currently, many works [1–3] have shown that in the case of a low-orbit SC, the most suitable for conducting experiments in the field of space materials science are a circular orbit and SC rest in the orbital coordinate system — orbital orientation. Depending on the conditions of the experiments, the orbital orientation of the SC can be realized both in the vicinity of its gravitationally stable equilibrium position and in an unstable one. In any case, maintaining such orientation requires the expenditure of energy or a working fluid.

One of the possible options for implementing spacecraft orbital orientation may be its passive orbital orientation, close to gravitationally stable, however, even in this case, due to the influence of the aerodynamic moment, it may turn out to be unstable and without proper correction cannot be maintained for a long time [4-5]. Or the level of microaccelerations on board the spacecraft will be unacceptable for conducting experiments. In this regard, to ensure long-term orbital orientation of the spacecraft in the presence of the destabilizing effect of the aerodynamic moment, damping devices can be used [6]. Gyroscopic actuators of the spacecraft control system

(gyrosystem) can be considered as such devices. To implement damping using a gyrosystem (so-called gyrodamping), it is sufficient to set an appropriate control law for the inherent kinetic moment of the gyrosystem (gyrostatic moment of the spacecraft). Such orbital orientation of the spacecraft can be called semi-passive, i.e., it can be considered active, but the energy costs for its maintenance are low. Additionally, gyrodamping can be implemented without accumulating the kinetic moment of the spacecraft, and there will be no energy or propellant costs for unloading the gyrosystem. Also, the need to unload the gyrosystem reduces the time of undisturbed spacecraft flight and imposes restrictions on the time of conducting experiments on board, therefore, implementing the orbital orientation mode without accumulating the gyrostatic moment of the spacecraft is a very significant advantage. The fundamental possibility of implementing gyrodamping is shown in the study [7]. In this paper, one of the possible variants of the gyrosystem control law is proposed, and the results of the numerical solution of the spacecraft motion equations are presented, confirming the possibility of implementing an orbital orientation mode using gyrodamping. Also, for the specified mode, an assessment of the level of quasi-static microaccelerations arising on board the spacecraft is carried out, and the results of their spectral analysis are shown.

Another possible option for spacecraft orientation for conducting space experiments on board is directly its orbital orientation in the vicinity of a gravitationally stable or unstable equilibrium position using a gyrosystem. As mentioned above, when using a gyrosystem, one of the criteria for its operational efficiency is the rate of accumulation of the gyrostatic moment. This rate determines the time intervals between gyrosystem unloadings and should be sufficiently small to provide prolonged segments of spacecraft flight with a low level of microaccelerations. The corresponding control laws implementing the orbital orientation of the spacecraft with simultaneous limitation of its gyrostatic moment growth were proposed in publications [7-10]. In this paper, one of the possible methods for selecting coefficients for each of the control laws considered in the article [8] is proposed, and the results of numerical solution of the spacecraft motion equations are presented, confirming the possibility of implementing the used control laws with the selected coefficient values.

All control laws proposed in this paper can be implemented for most spacecraft (including promising upper stages) that have a gyrosystem as part of their equipment, and for which it is required to maintain the orbital orientation mode in a low near-circular orbit for a long period of time without unloading the gyrostatic moment, which makes the task of implementing the modes considered in this paper quite relevant.

2. MATHEMATICAL MODELING OF MICROACCELERATIONS

Quasi-static microaccelerations on a low-orbit spacecraft are caused by four reasons: 1) spacecraft motion relative to the center of mass as a rigid body; 2) gravitational field gradient; 3) aerodynamic drag; 4) action of force created by control elements. If the spacecraft performs uncontrolled motion or a gyrosystem is used to control it, then the last of the listed reasons disappears. In such a case, the quasi-static microacceleration at a given fixed point on board is described by a simple formula, and to use it, it is sufficient to know only the orbit and rotational motion of the spacecraft.

Let the spacecraft represent a rigid body, and point P is rigidly attached to its frame. Microacceleration $\mathbf{b}$ at point P is defined as the difference between the gravitational field intensity at this point and the absolute acceleration of the latter. The role of vector $\mathbf{b}$ in orbital experiments is analogous to the role of free-fall acceleration in experiments on Earth's surface. In

particular, if a test body with negligibly small mass P , m_p is fixed at point then the reaction force acting on this body from the spacecraft will be equal to $-m_p\mathbf{b}$. The approximate formula for calculating microaccelerations has the form [11]

$$\left.\begin{aligned} \mathbf{b} &= \mathbf{b}_r + \mathbf{b}_g + \mathbf{b}_a, \\ \mathbf{b}_r &= \mathbf{d}\times\dot{\boldsymbol{\omega}} + (\boldsymbol{\omega}\times\mathbf{d})\times\boldsymbol{\omega}, \\ \mathbf{b}_g &= \frac{\mu_E}{r^3}\left(3\frac{\boldsymbol{\rho}\cdot\mathbf{r}}{r^2}\mathbf{r} - \boldsymbol{\rho}\right), \\ \mathbf{b}_a &= c\rho_a \mathrm{v}\,\mathbf{v}. \end{aligned}\right\}, \qquad (1)$$

Here $\boldsymbol{\rho}$ is the radius vector of point P relative to the center of mass of the spacecraft - point O ; $\boldsymbol{\omega}$ is the absolute angular velocity of the spacecraft; the dot above a letter denotes differentiation with respect to time t ; μ_E is the gravitational parameter of the Earth; $\mathbf{r}$ is the geocentric radius vector of point O , $r = |\mathbf{r}|$; $\mathbf{v}$ is the velocity of this point relative to the Earth's surface, $\mathrm{v} = |\mathbf{v}|$; ρ_a is the atmospheric density at point O ; c is the ballistic coefficient of the spacecraft. The terms on the right side of formula (1) correspond to the first three causes of microaccelerations mentioned above.

Formula (1) was used to calculate real quasi-static microaccelerations that occurred on spacecraft in flight [1, 2, 11]. It can also be used to predict microaccelerations [3, 12, 13]. In this case, equations of spacecraft motion are formulated, a motion mode is selected, the solution of the motion equations simulating this mode is calculated, and along the found solution, the microacceleration at a given point on board is calculated using formula (1). This is exactly how formula (1) is applied below.

3. EQUATIONS OF SPACECRAFT MOTION

The spacecraft is considered a gyrostat whose center of mass moves along a geocentric orbit. To describe its motion, we will use three right-handed Cartesian coordinate systems.

The coordinate system $Ox_1x_2x_3$ associated with the spacecraft is formed by its principal central axes of inertia. The origin of the system is at the center of mass of the spacecraft - point O. Somewhat simplifying the model, we assume that the axes of system $Ox_1x_2x_3$ are associated with characteristic elements of the spacecraft structure (fig. 1). Let us assume that the spacecraft has the shape of a right circular cylinder with radius R_c and height L_c with two identical rectangular plates - solar panels, with a total area of S_b . In order to minimize disturbances during experiments on board the spacecraft, it is planned to use solar panels without a special drive that orients the working surfaces of the panels relative to the Sun. The axis Ox_1 coincides with the axis of the cylinder. The solar panels are located in the plane Ox_1x_3 symmetrically with respect to the axis Ox_1 , the sides of the panels are parallel to the axes Ox_1 and Ox_3 , the axis Ox_2 is perpendicular to the plane of the solar panels. The coordinates of the geometric centers of the cylinder and the solar panel plates will be denoted as $(x_c,0,0)$ and $(x_b,0,0)$ respectively. Here and below, unless

otherwise specified, the components of vectors and coordinates of points refer to the system $Ox_1x_2x_3$. The basis unit vectors of the system $Ox_1x_2x_3$ will be denoted as $\mathbf{e}_1$, $\mathbf{e}_2$, $\mathbf{e}_3$.

Fig. 1. General shape of the spacecraft and position of the body-fixed coordinate system

In the orbital coordinate system $OX_1X_2X_3$, the axes OX_3 and OX_2 are directed along the geocentric radius vector of the point O and the vector of the angular momentum of the spacecraft's orbital motion, respectively. The basis unit vectors of this system will be denoted a $\mathbf{E}_1$, $\mathbf{E}_2$, $\mathbf{E}_3$.

The origin of the Greenwich coordinate system $O_{\mathrm{E}}Y_1Y_2Y_3$ is the point O_{E} located at the center of the Earth, the plane $O_{\mathrm{E}}Y_1Y_2$ coincides with the equatorial plane, the axis $O_{\mathrm{E}}Y_1$ intersects the Greenwich meridian, the axis $O_{\mathrm{E}}Y_3$ is directed along the Earth's rotation axis toward the North Pole. We assume that this system rotates with a constant angular velocity ω_{E} around the axis $O_{\mathrm{E}}Y_3$.

We denote the transition matrix from the orbital system to the Greenwich system as $W=(w_{ij})_{i,j=1}^{3}$, where w_{ij} is the cosine of the angle between the axes $O_{\mathrm{E}}Y_i$ and OX_j . The elements of this matrix are expressed through the components of the geocentric radius vector of the point O and the velocity vector of this point relative to the Earth's surface in the Greenwich coordinate system. The transition matrices from the system $Ox_1x_2x_3$ to the Greenwich and orbital systems will be denoted as $U=(u_{ij})_{i,j=1}^{3}$ and $Q=(q_{ij})_{i,j=1}^{3}$ respectively. Here $q_{ij}=\mathbf{E}_i\cdot\mathbf{e}_j$, u_{ij} and q_{ij} are the cosines of the angles that the axis Ox_j forms with the axes $O_{\mathrm{E}}Y_i$ and OX_i . The following relation holds: $U=WQ$.

The matrix Q is parameterized by angles γ, δ and β, , which are introduced as follows [3]. The system $Ox_1x_2x_3$ can be obtained from the system $OX_1X_2X_3$ by three consecutive rotations: 1) by angle $\delta+\pi/2$ around the axis OX_2 ; 2) by angle β around the new axis OX_3 ; 3) by angle γ around the axis OX_1, obtained after the first two rotations and coinciding with the axis Ox_1 . The elements of the matrix Q are expressed through these angles using the formulas

$$\left.\begin{aligned}
&q_{11}=-\sin\delta\cos\beta, \quad q_{12}=\cos\delta\sin\gamma+\sin\delta\sin\beta\cos\gamma\\
&q_{21}=\sin\beta, \qquad\qquad q_{22}=\cos\beta\cos\gamma,\\
&q_{31}=-\cos\delta\cos\beta, \quad q_{32}=-\sin\delta\sin\gamma+\cos\delta\sin\beta\cos\gamma,\\
&\\
&q_{13}=\cos\delta\cos\gamma-\sin\delta\sin\beta\sin\gamma,\\
&q_{23}=-\cos\beta\sin\gamma,\\
&q_{33}=-\sin\delta\cos\gamma-\cos\delta\sin\beta\sin\gamma.
\end{aligned}\right\} \qquad (2)$$

The spacecraft motion equations consist of two subsystems. One subsystem of equations for the vectors $\mathbf{r}$ and $\mathbf{v}$ describes the motion of the spacecraft's center of mass in the Greenwich

coordinate system, taking into account the non-central nature of Earth's gravitational field and atmospheric drag [14]. The non-central field is accounted for up to terms of order (16, 16) inclusive in the expansion of Earth's gravitational potential in a series of spherical functions. The atmosphere is considered to rotate with the Earth, and its density is calculated according to the GOST R 25645.166-2004 model. The atmospheric parameters and the spacecraft's ballistic coefficient are considered constant throughout the entire integration interval of the motion equations.

The other subsystem describes the spacecraft's motion relative to its center of mass (rotational motion) and has the form

$$\left.\begin{aligned} &\frac{\tilde{d}\,\mathbf{K}}{dt}+\boldsymbol{\omega}\times\mathbf{K}=\mathbf{M}_g+\mathbf{M}_a,\quad \mathbf{K}=\hat{I}\boldsymbol{\omega}+\mathbf{H},\\ &\frac{\tilde{d}\,\mathbf{u}_1}{dt}+\boldsymbol{\omega}\times\mathbf{u}_1=\omega_{\mathrm{E}}\mathbf{u}_2,\quad \frac{\tilde{d}\,\mathbf{u}_2}{dt}+\boldsymbol{\omega}\times\mathbf{u}_2=-\omega_{\mathrm{E}}\mathbf{u}_1. \end{aligned}\right\} \qquad (3)$$

Here, the symbol $\tilde{d}/dt$ denotes the local derivative of a vector in the system $Ox_1x_2x_3$; $\mathbf{K}$ — the angular momentum of the spacecraft in its motion relative to the center of mass; $\boldsymbol{\omega}=(w_1,w_2,w_3)^{\mathrm{T}}$ — the absolute angular velocity of the spacecraft; $\hat{I}=\mathrm{diag}(I_1,I_2,I_3)$ — the inertia tensor of the spacecraft; $\mathbf{H}=(h_1,h_2,h_3)^{\mathrm{T}}$ — the gyrostatic moment of the spacecraft (the intrinsic angular momentum of the gyro system); $\mathbf{M}_g$ — the gravitational moment acting on the spacecraft; $\mathbf{M}_a$ — the aerodynamic moment acting on the spacecraft; $\mathbf{u}_1$ and $\mathbf{u}_2$ — the first and second rows of the transition matrix U, respectively. The third row of this matrix is $\mathbf{u}_3=\mathbf{u}_1\times\mathbf{u}_2$. The rows $\mathbf{u}_1$ and $\mathbf{u}_2$ are related by the orthogonality conditions of the matrix U ($\mathbf{u}_i$ — unit vectors of the axes $O_{\mathrm{E}}Y_i$), which are taken into account when setting the initial conditions for these variables.

To close the subsystem of equations (3), we need to add an equation describing the change in the gyrostatic moment of the spacecraft in the form

$$\frac{\tilde{d}\,\mathbf{H}}{dt}+\boldsymbol{\omega}\times\mathbf{H}=-\mathbf{M}_c\ , \qquad (4)$$

where $\mathbf{M}_c$ — the moment acting from the gyro system on the spacecraft body. Expressions for $\mathbf{M}_c$ will be provided below.

The gravitational moment is given by the formula [15] $\mathbf{M}_g=3\frac{\mu_{\mathrm{E}}}{r^5}(\mathbf{r}\times\hat{I}\mathbf{r})$.

The formula for the aerodynamic moment is given by

$$\mathbf{M}_a=p\left(\mathbf{v}\times\mathbf{e}_1\right)\ ,\ p=\rho_a\left(\pi R_c^2 y_c\,|\,\mathrm{v}_1\,|+S_b y_b\,|\,\mathrm{v}_2\,|+2R_c L_c y_c\sqrt{\mathrm{v}_2^2+\mathrm{v}_3^2}\right),$$

where v_i are components of the vector $\mathbf{v}$, $i=\overline{1,3}$. When deriving the last formula, it was assumed that atmospheric molecules experience a completely inelastic collision when hitting the spacecraft body [16], and the mutual shadowing of the spacecraft body and solar panels from the incoming aerodynamic flow was not taken into account. Such simplification is justified because for most spacecraft movements, the relative duration of time intervals in which this shadowing is significant is small.

Let us present the numerical values of the parameters of the described model used in calculations. Spacecraft parameters: $m = 6440$ kg, $I_1 = 2600$ kg m^2, $I_2 = 11100$ kg m^2, $I_3 = 10900$ kg m^2, $R_c = 1.3$ m, $L_c = 5.0$ m, $S_b = 33$ m^2, $x_b = -1$ m, $x_c = 0.3$ m. The initial conditions for the spacecraft center of mass motion were specified at the ascending node of the orbit at 09:10:34 UTC on 21.IX.2007. Initial orbital elements: apogee altitude 450 km, perigee altitude 400 km, inclination 63.0°, argument of perigee latitude 53.5°, longitude of the ascending node (measured from the mean vernal equinox of the date epoch) 164.0°. Microaccelerations were calculated at the point P with coordinates (–1 m, 0.7 m, 0.5 m) (Fig. 1). This point is located on the inner wall of the spacecraft working compartment, approximately at its middle. Scientific equipment can be installed near this point. Atmospheric model parameters: $F_{10.7} = F_{81} = 150$, $A_p = 12$.

The initial conditions for equations (3) were set at the same time as the initial conditions for the orbital motion. This moment served as the time reference point — point $t = 0$.

4. ORBITAL ORIENTATION MODE OF A SPACECRAFT USING GYRODAMPING

First, let's consider the gravitational orientation mode of a spacecraft. Equations (3) are inconvenient for explaining such a mode and the method of its implementation, but this can be done using simpler equations that take into account only the main factors. Let's assume that the orbit of the spacecraft's center of mass is circular and unchanged in absolute space, and only gravitational torque acts on the spacecraft. In this case, equations (3) can be transformed to the form

$$\begin{cases} \hat{I}\dot{\boldsymbol{\omega}} + \dot{\mathbf{H}} + \boldsymbol{\omega} \times (\hat{I}\boldsymbol{\omega} + \mathbf{H}) = 3\omega_0^2 \left(\mathbf{E}_3 \times \hat{I}\mathbf{E}_3 \right), \\ \dot{\gamma} = \omega_1 - \operatorname{tg}\beta \left(\omega_2 \cos\gamma - \omega_3 \sin\gamma \right), \\ \dot{\delta} = \dfrac{\omega_2 \cos\gamma - \omega_3 \sin\gamma}{\cos\beta} - \omega_0, \\ \dot{\beta} = \omega_2 \sin\gamma + \omega_3 \cos\gamma. \end{cases} \qquad (5)$$

In this case, system (5) has 24 stationary solutions in which $\boldsymbol{\omega} = \omega_0 \mathbf{E}_2$, the unit vectors $\mathbf{e}_i$ coincide with the unit vectors $\pm\mathbf{E}_j$, $i, j = \overline{1,3}$, where $\omega_0 = \sqrt{\mu_E / r^3}$ is the mean motion of the spacecraft (orbital frequency). These solutions describe the equilibrium positions (rest) of the spacecraft in the orbital coordinate system [15]. Here $\mathbf{E}_3 = \left(q_{31}, q_{32}, q_{33} \right)^{\mathrm{T}}$, and the values q_{3i} are expressed through the angles γ, δ and β by formulas (2).

We shall limit ourselves to considering two stationary solutions of the system (5), given by the relations:

$$\mathbf{e}_1 = -\mathbf{E}_3,\ \mathbf{e}_2 = \mathbf{E}_2,\ \mathbf{e}_3 = \mathbf{E}_1, \qquad (6)$$

$$\mathbf{e}_1 = \mathbf{E}_1,\ \mathbf{e}_2 = \mathbf{E}_3,\ \mathbf{e}_3 = -\mathbf{E}_2\ . \qquad (7)$$

When the inequalities $I_1 < I_3 < I_2$ are satisfied, solution (6) is stable, and solution (7) is unstable [15]. The stable stationary solution (6) can be used to implement a passive three-axis gravitational orientation mode of the spacecraft. Further in the text, the stable equilibrium position (6) will be called the gravitational orientation of the spacecraft.

To implement gyrodamping for the orbital orientation mode of the spacecraft, close to its gravitational orientation, we define the law of change of the intrinsic kinetic moment of the gyrosystem in the form [7]

$$\hat{T}\dot{\mathbf{H}} + \mathbf{H} - h_0\mathbf{e}_2 = \hat{J}\left(\boldsymbol{\omega} - \omega_0\mathbf{e}_2\right), \qquad (8)$$

where $\hat{T} = \mathrm{diag}(\tau_1, \tau_2, \tau_3)$; $\hat{J} = \mathrm{diag}(J_1, J_2, J_3)$; J_i, τ_i, $i = \overline{1,3}$ are positive constants; h_0 is an arbitrary constant. Using the control law (8) for the rotational motion of the spacecraft implies the presence of angular velocity sensors on board, according to the readings of which the intrinsic kinetic moment of the gyrosystem changes.

The system of equations (5), (8) admits a stationary solution

$$\gamma = \delta = \beta = 0,\ \omega_1 = \omega_2 - \omega_0 = \omega_3 = 0,\ h_1 = h_2 - h_0 = h_3 = 0. \quad (9)$$

This solution also describes the equilibrium position of the spacecraft in the orbital coordinate system, while the orientation of the system axes $Ox_1x_2x_3$ corresponds to the relations (6). To study the stability of the stationary solution (9), one can use the theorems of E.A. Barbashin and N.N. Krasovsky [17]. Let's consider the Lyapunov function [7]

$$V = \frac{1}{2}\sum_{i=1}^{3} I_i\omega_i^2 - \omega_0\sum_{i=1}^{3} I_i\omega_i q_{2i} + \frac{3}{2}\omega_0^2\sum_{i=1}^{3} I_i q_{3i}^2 + \omega_0\left(h_2 - \sum_{i=1}^{3} h_i q_{2i}\right) + \frac{1}{2}\omega_0^2\left(I_2 - 3I_1\right) + \\ + \frac{1}{2}\left(\frac{h_1^2}{J_1} + \frac{\left(h_2 - h_0\right)^2}{J_2} + \frac{h_3^2}{J_3}\right).$$

Its derivative by virtue of the system (5), (8)

$$\dot{V} = -\left(\sum_{i=1}^{3}\frac{\tau_i\dot{h}_i^2}{J_i}\right)$$

is sign-negative.

In the vicinity of the solution (9) with accuracy up to third-order terms of smallness with respect to $\gamma, \delta, \beta,\ \omega_1, \omega_2 - \omega_0, \omega_3,\ h_1, h_2 - h_0, h_3$ we have

$$V = \frac{I_1}{2}\left(\omega_1 - \omega_0\beta\right)^2 + \frac{I_2}{2}\left(\omega_2 - \omega_0\right)^2 + \frac{I_3}{2}\left(\omega_3 + \omega_0\gamma\right)^2 + \frac{1}{2}\left[\left(I_2 - I_3\right)\omega_0 + h_0\right]\omega_0\gamma^2 + \\ + \frac{3}{2}\omega_0^2\left(I_3 - I_1\right)\delta^2 + \frac{1}{2}\left[4\left(I_2 - I_1\right)\omega_0 + h_0\right]\omega_0\beta^2 + \omega_0\left(h_3\gamma - h_1\beta\right) + \\ + \frac{1}{2}\left(\frac{h_1^2}{J_1} + \frac{\left(h_2 - h_0\right)^2}{J_2} + \frac{h_3^2}{J_3}\right).$$

The non-trivial conditions for positive definiteness of the written quadratic form are expressed by the inequalities

$$\left(I_2 - I_3 - J_3\right)\omega_0 + h_0 > 0,\ \left[4\left(I_2 - I_1\right) - J_1\right]\omega_0 + h_0 > 0,\ I_3 > I_1. \qquad (10)$$

If the latter inequalities are satisfied and

$$I_2 \neq I_1, \qquad (11)$$

then the intersection of the set $\dot{V} = 0$ with a sufficiently small neighborhood of the equilibrium position (9) does not contain entire trajectories of the system (5), (8) other than expressions (9). This statement is established by the method described in publication [18], through analysis of the

corresponding linearized equations. When inequalities (10), (11) are satisfied, the conditions of the Barbashin - Krasovsky theorem ([17], theorem 3.2) are met and the equilibrium position (9) is asymptotically stable. If at least one of the inequalities (10) is satisfied with the opposite sign and inequality (11) still holds, then the conditions of Krasovsky's theorem ([17], theorem 4.1) are satisfied and the equilibrium position (9) is unstable [7].

Due to various disturbing factors (orbit ellipticity, influence of aerodynamic moment, etc.), the system of equations (3) for the considered spacecraft does not have solutions describing its rest (9) in the orbital coordinate system, however, due to the continuous dependence of the solutions of differential equations on initial conditions and parameters, these equations admit solutions which, after recalculating the variables u_{1i}, u_{2i}, $i=\overline{1,3}$ into angles γ, δ and β will be close to the rest position (9).

5. CONTROL OF THE ROTATIONAL MOTION OF A SPACECRAFT

To implement the control law (8), we express the moment $\mathbf{M}_c$ acting from the gyro system on the spacecraft body and stabilizing the gravitational orientation mode of the spacecraft in the vicinity of position (9) in the form

$$\mathbf{M}_c = \mathbf{H}\times\boldsymbol{\omega} - \hat{T}^{-1}\hat{J}\left(\boldsymbol{\omega}-\omega_0\mathbf{e}_2\right)+\hat{T}^{-1}\left(\mathbf{H}-h_0\mathbf{e}_2\right)\ . \qquad (12)$$

The system (4), (5), (12), linearized in the vicinity of the stationary solution (9) splits into two independent subsystems, which have the form

$$\dot{\mathbf{x}}_1=\left(A_1+B_1K_1\right)\mathbf{x}_1,\ \mathbf{x}_1=\left(\omega_2-\omega_0,\delta,h_2-h_0\right)^{\mathrm{T}}, \qquad (13)$$

$$A_1=\begin{pmatrix}0 & 3\omega_0^2\left(I_1-I_3\right)/I_2 & 0\\ 1 & 0 & 0\\ 0 & 0 & 0\end{pmatrix}\ B_1=\left(1/I_2,0,-1\right)^{\mathrm{T}},\ K_1=\left(-J_2/\tau_2,0,1/\tau_2\right),$$

$$\dot{\mathbf{x}}_2=\left(A_2+B_2K_2\right)\mathbf{x}_2,\ \mathbf{x}_2=\left(\omega_1,\omega_3,\gamma,\beta,h_1,h_3\right)^{\mathrm{T}}, \qquad (14)$$

$$A_2=\begin{pmatrix}0 & \left(\omega_0\left(I_2-I_3\right)+h_0\right)/I_1 & 0 & 0 & 0 & -\omega_0/I_1\\ \left(\omega_0\left(I_1-I_2\right)-h_0\right)/I_3 & -J_3/I_3\tau_3 & 0 & 3\omega_0^2\left(I_1-I_2\right)/I_3 & \omega_0/I_3 & 0\\ 1 & 0 & 0 & -\omega_0 & 0 & 0\\ 0 & 1 & \omega_0 & 0 & 0 & 0\\ 0 & 0 & 0 & 0 & 0 & 0\\ 0 & 0 & 0 & 0 & 0 & 0\end{pmatrix},$$

$$B_2 = \begin{pmatrix} 1/I_1 & 0 & 0 & 0 & -1 & 0 \\ 0 & 1/I_3 & 0 & 0 & 0 & -1 \end{pmatrix}^{\mathrm{T}},\ K_2 = \begin{pmatrix} -J_1/\tau_1 & 0 & 0 & 0 & 1/\tau_1 & 0 \\ 0 & -J_3/\tau_3 & 0 & 0 & 0 & 1/\tau_3 \end{pmatrix}$$

The structure of matrices K_1, K_2 implies that information about the spacecraft's orientation is not required to form the control of its rotational motion. We will choose the values of coefficients J_i, τ_i, $i = \overline{1,3}$ in such a way that all roots of the characteristic polynomial of the linearized system lie in the left half-plane of the complex variable sufficiently far from the imaginary axis. More precisely, we will consider the quality criterion of the control law (12) to be the degree of stability of the linearized system (13), (14) — the negative real part of the rightmost root of its characteristic polynomial. In this case, this polynomial decomposes into polynomials of the third

$$\det\left[\left(A_1 + B_1K_1\right) - \lambda^{(1)}E_3\right] = 0\ ,$$

and sixth orders

$$\det\left[\left(A_2 + B_2K_2\right) - \lambda^{(2)}E_6\right] = 0\ ,$$

which are the characteristic polynomials of the first (13) and second subsystems (14) respectively. Here E_3 and E_6 are identity matrices of the third and sixth orders respectively.

The third-order polynomial depends on the coefficients J_2, τ_2. We choose them so that this polynomial has a triple real root $\lambda_j^{(1)} = -\alpha$, $j = \overline{1,3}$ where $\alpha > 0$ is the degree of stability. We get

$$\tau_2 = \frac{3}{\alpha},\ J_2 = 8I_2,\ \alpha = \omega_0\sqrt{\frac{I_3 - I_1}{I_2}}\ .$$

From the given relations, it is evident that the maximum degree of stability of the first subsystem (13) is determined only by the moments of inertia of the spacecraft and the height of its orbit. For the spacecraft under consideration

$$\omega_0 = 1.125\cdot10^{-3}\ \text{с}^{-1},\ \alpha = 9.73\cdot10^{-4}\ \text{с}^{-1},\ \tau_2 = 3084\ \text{с},\ J_2 = 88000\ \text{кг м}^2.$$

The sixth-order polynomial contains coefficients t_1, J_1 and t_3, J_3. Taking into account the relations (10) for the asymptotic stability of system (14), the following conditions must be met:

$$0 < J_1 < \left(4\left(I_2 - I_1\right) + \frac{h_0}{\omega_0}\right),\ 0 < J_3 < \left(I_2 - I_3 + \frac{h_0}{\omega_0}\right).\ (15)$$

Taking the value h_0 = 5 N m s, we find the values of J_1, J_3 in the form

$$J_1 = \frac{1}{2}\left(4\left(I_2 - I_1\right) + \frac{h_0}{\omega_0}\right) = 19222\ \text{kg m}^2,\ J_3 = \frac{1}{2}\left(I_2 - I_3 + \frac{h_0}{\omega_0}\right) = 2322\ \text{kg m}^2.$$

Let's take the values

$$\tau_1 = J_1/\chi_1 = 4805\ \text{с},\ \tau_3 = J_3/\chi_3 = 2322\ \text{s},$$

where $\chi_1 = 4$ N m s, $\chi_3 = 1$ N m s. The roots of the sixth-order polynomial are equal to

$$\lambda_{1,2}^{(2)} = -1.37\cdot10^{-4} \pm 2.0\cdot10^{-3}i\ \text{с}^{-1},\ \lambda_{3,4}^{(2)} = -1.37\cdot10^{-4} \pm 3.7\cdot10^{-5}i\ \text{с}^{-1},$$

$$\lambda_{5,6}^{(2)} = -8.61 \cdot 10^{-4} \pm 1.4 \cdot 10^{-3} i \ \text{c}^{-1}.$$

The degree of stability of the sixth-order polynomial $\alpha = 1.37 \cdot 10^{-4}$ s^{-1}. Thus, the control law (12) with the specified parameter values J_i, τ_i, $i = \overline{1,3}$ ensures the asymptotic stability of the system (3), (4) in the neighborhood of the stationary solution (9).

6. MATHEMATICAL MODELING OF THE ORBITAL ORIENTATION MODE OF A SPACECRAFT USING GYRO DAMPING

Let's show that the chosen law of change for the control moment of the gyro system (12) indeed provides stable orientation of the spacecraft, close to gravitational. For this purpose, we will calculate the solutions of the system (3), (4), (12) with initial conditions $\gamma(0) = \delta(0) = \beta(0) = 0$, $h_1(0) = h_3(0) = 5$ N m s, $h_2(0) = 0$ and

$$\omega_1(0) = \omega_2(0) - \omega_0 = \omega_3(0) = 0.01 \ ^\circ/\text{s} \qquad (16)$$

over a time interval of 140 days. The values of the corresponding coefficients of the control law (12) are taken as in the section "Control of spacecraft rotational motion". In Fig. 2-4 show the graphs of time dependence of angles γ, δ, β, components h_i, $i = \overline{1,3}$ and the module of the gyrostatic moment $|\mathbf{H}|$, as well as components b_i, $i = \overline{1,3}$ and the module $|\mathbf{b}|$ of the microacceleration vector. The graphs do not show the initial segment with a duration of 1 day, containing the transient process caused by errors in setting the initial angular velocity (16) and initial values of the gyrostatic moment. The calculation results show that the control law (12) provides stable orbital orientation of the spacecraft, and the gyrostatic moment remains limited. In the steady state, the amplitudes of oscillations of the angular velocity components are limited by the following values:

$$|\omega_1| < 6 \cdot 10^{-5} \ ^\circ/\text{s}, \ |\omega_2 - \omega_0| < 2 \cdot 10^{-3} \ ^\circ/\text{s}, \ |\omega_3| < 3 \cdot 10^{-4} \ ^\circ/\text{s}.$$

Due to the selected time scale in Fig. 2-4, oscillations of the corresponding values with frequencies multiple of ω_0 caused by atmospheric drag and orbit ellipticity are not visible. Such oscillations are shown in [3], where results of numerical solution of the spacecraft motion equations with a similar control law are presented for a time interval of 6 days.

Fig. 2. Spacecraft orientation angles when using control law (12)

Fig. 3. Components and module of the spacecraft gyrostatic moment vector when using control law (12)

Fig. 4. Components and module of the spacecraft microacceleration vector

In Fig. 2, the increase in oscillation amplitude, as well as the constant offset of angle $\delta \approx 0.8°$ are caused by atmospheric drag, which depends on the position of the Sun relative to the spacecraft's orbital plane. This position changes due to the precession of the orbital plane with

an angular velocity of ~5 °/day. Over a period of approximately 70 days, the value of the constant offset of angle δ practically does not change, the oscillation amplitude varies in the range from 0.1 to 1.5°. Since the control law (12) does not impose restrictions on the angular position of the spacecraft, the values of angles γ, δ, β, shown in Fig. 2, at each moment of time correspond to a certain relative equilibrium position of the spacecraft under the action of gravitational and aerodynamic moments [19]. One of the possible methods of finding such a position is presented in publication [8]. In this case, to estimate the displacement δ_0 of the angle value δ an approximate analytical dependence

$$\delta_0 = \frac{2R_c L_c x_c (R_0 + R_E)^2 \rho_a}{3(I_3 - I_1) + \pi R_c^2 x_c (R_0 + R_E)^2 \rho_a},$$

can be used, which was obtained by linearizing the system (3) in the vicinity of the stationary solution (9). In this linearization, it was assumed that the center of mass of the spacecraft moves along a circular orbit of radius $r = R_0 + R_E$, unchangeable in absolute space, and the incident flow velocity is directed tangentially to the spacecraft's orbit [20]. Here $R_E = 6378.14$ km is the radius of the Earth taken as a sphere, R_0 is the height of the spacecraft's circular orbit. Table 1 shows some values of δ_0 depending on the values of R_0. The corresponding R_0 values of atmospheric density ρ_a were taken from GOST R 25645.166-2004 for $F_{10.7} = 150$.

Table 1

R_0, km	400	420	440
ρ_a, kg/m^3	$3.02 \cdot 10^{-12}$	$2.11 \cdot 10^{-12}$	$1.48 \cdot 10^{-12}$
δ_0, deg	1.101	0.801	0.580

In Fig. 3, the displacement of the component h_2 and the modulus $|\mathbf{H}|$ of the gyrostatic moment vector is determined by the value of the constant h_0 = 5 N·m·s of the control law (12). As can be seen from the inequalities (15), the value h_0 affects the size of the stability region of the coefficients J_1, J_3, the larger the value of h_0, the larger the size of this region. However, when choosing the value of h_0, the specific characteristics and layout of the gyrosystem actuators installed on board the spacecraft should be taken into account, so that during the implementation of the control law, the intrinsic kinetic moment of each actuator does not approach its limit value [20].

Figure 4 shows that the value of the micro-acceleration vector modulus $|\mathbf{b}|$ does not exceed $4.1 \cdot 10^{-6}$ m/s^2, and the variation region of the vector $\mathbf{b}$ is relatively small. It should be noted that the value $|\mathbf{b}| < 10^{-5}$ m/s^2 is acceptable when conducting space experiments, particularly in the field of materials science [21]. The small size of the vector variation region $\mathbf{b}$ ($|\mathbf{b}| \approx |b_1|$) is an additional advantage of the spacecraft's gravitational orientation mode when conducting these experiments.

7. SPECTRAL ANALYSIS OF MICRO-ACCELERATIONS

To analyze the level of micro-accelerations occurring on board the spacecraft during the implementation of the control law (12), the paper defines the characteristic oscillation frequencies of the vector moduli $\mathbf{b}_a$, $\mathbf{b}_g$ and $\mathbf{b}$ (1). The frequencies were found using spectral analysis, performed according to the following scheme [22]. Let x_n, $n=\overline{1,N}$ be the values of some variable $x(t)$ of the solution under study at the nodes of a uniform time grid $\{t_n\}$: $x_n = x(t_n)$. In all examples considered below, the grid step is $h = t_{n+1} - t_n = 10$ s. Suppose that the function under study has the form

$$x(t) = \alpha_0 + \sum_{k=1}^{M} (\alpha_m \cos 2\pi f_m^\circ t + \beta_m \sin 2\pi f_m^\circ t) ,$$

where $f_m^\circ \in (0, h^{-1}/2)$ and α_0, α_m, β_m, $m=\overline{1,M}$ are constant parameters, and there are no identical frequencies among f_m°. The frequencies and amplitudes of individual harmonics in $x(t)$ can be estimated by examining the maxima of the Schuster periodogram —

$$I(f) = \left[\sum_{n=1}^{N} (x_n - x_*)\cos 2\pi f t_n\right]^2 + \left[\sum_{n=1}^{N} (x_n - x_*)\sin 2\pi f t_n\right]^2, \quad x_* = \frac{1}{N}\sum_{n=1}^{N} x_n ,$$

in the interval $0 < f < h^{-1}/2$. The function $I(f)$ has many maxima, from which several of the most prominent ones are selected. If the function $I(f)$ has such a maximum at the point f_*, it is assumed that f_* is close to one of the frequencies f_m°, and the value $2\sqrt{I(f_*)}/N$ is an estimate of the amplitude $\sqrt{\alpha_m^2 + \beta_m^2}$ of the corresponding harmonic. The Schuster periodogram can be conveniently transformed into a form called the amplitude spectrum $A(f) = 2N^{-1}\sqrt{I(f)}$. The prominent maxima of the function $A(f)$ directly estimate the amplitudes of individual harmonics, but its maxima are less visually pronounced than the maxima of the periodogram.

In Fig. 5 shows the amplitude spectra $A_{\mathbf{ba}}(f)$, $A_{\mathbf{bg}}(f)$, $A_{\mathbf{b}}(f)$ of values $|\mathbf{b}_a|$, $|\mathbf{b}_g|$ and $|\mathbf{b}|$ respectively. The spectra are presented in the frequency range from 0 to 0.001 Hz, with values $h = 10$ s and $N = 6.048 \cdot 10^6$. It is shown that the greatest contribution to the overall level of micro-accelerations $\mathbf{b}$ on board the spacecraft when using the law (12) is made by the component $\mathbf{b}_a$ with the dominant frequency $f_0 = \omega_0/2\pi \approx 1.79 \cdot 10^{-4}$ Hz. Such oscillations are caused by the influence of the atmosphere. There is also an increase in the oscillation amplitudes of the values $|\mathbf{b}_a|$ and $|\mathbf{b}|$ at the frequency $2f_0 \approx 3.58 \cdot 10^{-4}$ Hz, however, such an increase in amplitudes practically does not affect the overall level of micro-accelerations occurring on board $\mathbf{b}$.

Fig. 5. Amplitude spectra of the moduli of vectors $\mathbf{b}_a$, $\mathbf{b}_g$ and $\mathbf{b}$

Considering the overall level of micro-accelerations shown in Fig. 4, the small variation area of the vector **b** and that the micro-acceleration oscillations occur very slowly - with orbital frequency, it can be stated that the conditions on board the spacecraft are acceptable for conducting space experiments [3, 11].

8. ORBITAL ORIENTATION OF THE SPACECRAFT IN THE VICINITY OF THE GRAVITATIONALLY STABLE EQUILIBRIUM POSITION

The control law (8) can be implemented without using a constant value of the gyrostatic moment h_0 . Let's denote the equilibrium position (9) at $h_0 = 0$ as (9′). Then the moment $\mathbf{M}_c$, acting from the gyro system on the spacecraft body and stabilizing the gravitational orientation mode of the spacecraft in the vicinity of the equilibrium position (9′), can be represented as [8]

$$\mathbf{M}_c = -K_\omega(\boldsymbol{\omega} - \omega_0 \mathbf{e}_2) + K_h \mathbf{H} \ , \qquad (17)$$

where $K_\omega = (k_{ij}^{(\omega)})_{i,j=1}^3$, $K_h = (k_{ij}^{(h)})_{i,j=1}^3$, $k_{ij}^{(\omega)}$, $k_{ij}^{(h)}$, $i, j = \overline{1,3}$ are constant values. The system (4), (5), (17), linearized in the vicinity of the solution (9′), can be represented as two independent subsystems of the third and sixth order [23]:

$$\dot{\mathbf{x}}_3 = \left(A_3 + B_3 K_3 C_3\right)\mathbf{x}_3, \ \mathbf{x}_3 = \left(\omega_2 - \omega_0, \delta, h_2\right)^{\mathrm{T}}, \qquad (18)$$

$$A_3 = \begin{pmatrix} 0 & 3\omega_0^2\left(I_1 - I_3\right)/I_2 & 0 \\ 1 & 0 & 0 \\ 0 & 0 & 0 \end{pmatrix}, \ B_3 = \left(1/I_2, 0, -1\right)^{\mathrm{T}}, \ C_3 = \mathrm{diag}\left(1,0,1\right), \ K_3 = \left(-k_{22}^{(\omega)}, 0, k_{22}^{(h)}\right),$$

$$\dot{\mathbf{x}}_4 = \left(A_4 + B_4 K_4 C_4\right)\mathbf{x}_4 \ , \ \mathbf{x}_4 = \left(\omega_1, \omega_3, \gamma, \beta, h_1, h_3\right)^{\mathrm{T}} \ , \quad (19)$$

$$A_4 = \begin{pmatrix} 0 & \omega_0\left(I_2 - I_3\right)/I_1 & 0 & 0 & 0 & 0 \\ \omega_0\left(I_1 - I_2\right)/I_3 & 0 & 0 & 3\omega_0^2\left(I_1 - I_2\right)/I_3 & 0 & 0 \\ 1 & 0 & 0 & -\omega_0 & 0 & 0 \\ 0 & 1 & \omega_0 & 0 & 0 & 0 \\ 0 & 0 & 0 & 0 & 0 & -\omega_0 \\ 0 & 0 & 0 & 0 & \omega_0 & 0 \end{pmatrix},$$

$$B_4 = \begin{pmatrix} 1/I_1 & 0 & 0 & 0 & -1 & 0 \\ 0 & 1/I_3 & 0 & 0 & 0 & -1 \end{pmatrix}^{\mathrm{T}} \ , \ C_4 = \mathrm{diag}\left(1,1,0,0,1,1\right) \ ,$$

$$K_4 = \begin{pmatrix} -k_{11}^{(\omega)} & -k_{13}^{(\omega)} & 0 & 0 & k_{11}^{(h)} & k_{13}^{(h)} \\ -k_{31}^{(\omega)} & -k_{33}^{(\omega)} & 0 & 0 & k_{31}^{(h)} & k_{33}^{(h)} \end{pmatrix}.$$

In this case, as in section 5, the structure of matrices K_3, C_3, K_4, C_4 implies that information about the spacecraft's orientation is not required to form the control of the rotational movement of the spacecraft. In this case $k_{12}^{(\omega)} = k_{21}^{(\omega)} = k_{23}^{(\omega)} = k_{32}^{(\omega)} = 0$ and $k_{12}^{(h)} = k_{21}^{(h)} = k_{23}^{(h)} = k_{32}^{(h)} = 0$.

The characteristic polynomial of the third-order system depends on coefficients $k_{22}^{(\omega)}$ and $k_{22}^{(h)}$. Let's choose them as in section 5, so that this polynomial has a triple real root $\lambda_j^{(3)} = -\alpha$, $j = \overline{1,3}$ where $\alpha > 0$ is the degree of stability. We obtain analytical dependencies

$$k_{22}^{(h)} = \frac{\alpha}{3}, \quad k_{22}^{(\omega)} = \frac{8 I_2 \alpha}{3}, \quad \alpha = \omega_0 \sqrt{\frac{I_3 - I_1}{I_2}}.$$

For the considered spacecraft: $k_{22}^{(h)} =$ 3.24·10^{-4} s^{-1}, $k_{22}^{(\omega)} =$ 28.8 N·m·s.

The values of the coefficients of the sixth-order polynomial will be found as a solution to the linear-quadratic regulation problem [24] in the form $K_4 = -S^{-1} B_4^{\mathrm{T}} P$, where $P \in \mathbb{R}^{6\times 6}$ is the matrix obtained as a result of numerical solution of the algebraic Riccati matrix equation

$$P A_4 + A_4^{\mathrm{T}} P - P B_4 S^{-1} B_4^{\mathrm{T}} P + C_4{}^{\mathrm{T}} R C_4 = 0 \ . \qquad (20)$$

Here $R \in \mathbb{R}^{6\times 6}$ and $S \in \mathbb{R}^{2\times 2}$ are positive definite matrices of weight coefficients, whose chosen values $R = \mathrm{diag}\left(1{,}5\cdot 10^7, 0, 0, 100, 1\right)$, $S = \mathrm{diag}\left(1,1\right)$ correspond to coefficient values

$k_{11}^{(\omega)} =$ 1042.76 N·m·s, $k_{13}^{(\omega)} =$ –1271.81 N·m·s, $k_{11}^{(h)} =$ 9.60 s^{-1}, $k_{13}^{(h)} =$ 0.12 s^{-1},
$k_{31}^{(\omega)} =$ 6620.91 N·m·s, $k_{33}^{(\omega)} =$ –3709.13 N·m·s, $k_{31}^{(h)} =$ –2.55 s^{-1}, $k_{33}^{(h)} =$ 1.54 s^{-1}.

The corresponding values of the roots of the sixth-degree characteristic polynomial

$\lambda_{1,2}^{(4)} =$ –1.03·10^{-4} ± 2.10·10^{-3} i s^{-1}, $\lambda_{3,4}^{(4)} =$ –1.14·10^{-3} ± 4.72·10^{-4} i s^{-1},
$\lambda_5^{(4)} =$ –1.20 s^{-1}, $\lambda_6^{(4)} =$ –10.00 s^{-1}.

The degree of stability of a sixth-order polynomial $\alpha =$ 1.03·10^{-4} s^{-1}. Thus, the control law (17), with the specified parameter values $k_{ij}^{(\omega)}$, $k_{ij}^{(h)}$, $i, j = \overline{1,3}$, ensures asymptotic stability of the system (3), (4) in the neighborhood of the stationary solution (9′). The presented values of the matrix elements R and S, as well as the method used to find the control law coefficients in general, are not the only possible ones. By applying special methods from the mathematical theory of automatic control [24], it is probably possible to obtain values of the sixth-order polynomial coefficients that provide a greater stability margin and better control quality. However, this represents a topic for separate research.

It should be noted that the control law (17) is essentially the control law (12), in which the term v is not taken into account, the value $h_0 = 0$ is used, and different notations are used for the coefficients: $K_\omega = \hat{T}^{-1}J$, $K_h = \hat{T}^{-1}$. Therefore $A_3 = A_1$, $B_3 = B_1$, $B_4 = B_2$ and matrices A_4, A_2 have a similar structure. The introduction of new notations was done to present the linearized system of equations in the form (18), (19) for the convenience of numerically solving equation (20). Thus, the coefficients of the control law (12) ensuring asymptotic stability of the system (3), (4) in the neighborhood of the stationary solution (9) can also be selected as a result of solving the linear-quadratic regulation problem using the corresponding matrices of the linearized system (14).

Let us show that for the found coefficient values $k_{ij}^{(\omega)}$, $k_{ij}^{(h)}$, $i, j = \overline{1,3}$ the law of change of the gyrosystem control moment (17) indeed provides stable orientation of the spacecraft, close to gravitational. For this, we will calculate solutions of the system (3), (4), (17) with initial conditions $\gamma(0) = \delta(0) = \beta(0) = 0$, $h_1(0) = h_2(0) = h_3(0) = 0$ and (16) over a time interval of 8 days. In Fig. 6, 7 show graphs of the time dependence of angles γ, δ, β, components h_i, $i = \overline{1,3}$ and the modulus of the gyrostatic moment $|\mathbf{H}|$. The graphs do not show the initial section lasting 1 day, containing the transient process, which is caused by errors in setting the initial angular velocity (16). The calculation results show that the control law (17) provides stable orbital orientation of the spacecraft, and the gyrostatic moment remains limited. In the steady state, the oscillation amplitudes of the angular velocity components are limited by the following values:

$$|\omega_1| < 8\cdot10^{-5}\,°/\text{s},\ |\omega_2| < 2\cdot10^{-3}\,°/\text{s},\ |\omega_3| < 2\cdot10^{-4}\,°/\text{s}.$$

Fig. 6. Spacecraft orientation angles when using control law (17)

Fig. 7. Components and modulus of the spacecraft gyrostatic moment vector when using control law (17)

In Fig. 6, an increase in the oscillation amplitude of the angle δ is noticeable, as well as its constant offset, which fully corresponds to the results presented in section 6 in Fig. 2. The absence of a term containing a constant value of the gyrostatic moment h_0 in the control law (17) does not significantly affect the angular orientation of the spacecraft, its absolute angular velocity, and the level of micro-accelerations on board; the difference is visible only in the gyrostatic moment graphs. In Fig. 7, it can be seen that when using the control law (17), there is no constant offset in the component h_2 and modulus $|\mathbf{H}|$. The established oscillations of the values γ, δ, β, ω_i, h_i, $i = \overline{1,3}$ and $|\mathbf{H}|$ occur with a dominant frequency equal to the orbital frequency ω_0, which corresponds to the influence of aerodynamic drag $c\rho_a v\mathbf{v}$.

9. ORBITAL ORIENTATION OF A SPACECRAFT IN THE VICINITY OF A GRAVITATIONALLY UNSTABLE EQUILIBRIUM POSITION

Let us consider the stationary solution (7) of system (5), which, when the inequalities $I_1 < I_3 < I_2$ are satisfied, will be unstable. To implement the orbital orientation mode of the spacecraft in the vicinity of a gravitationally unstable equilibrium position, we define the control law for the gyro system in the form [8]

$$\mathbf{M}_c = -K_\theta\left[\left(\mathbf{E}_3 \times \mathbf{e}_2\right) + \left(\mathbf{e}_3 \times \mathbf{E}_2\right)\right] - K_\omega\left(\boldsymbol{\omega} - \omega_0 \mathbf{E}_2\right) + K_h \mathbf{H}, \quad (21)$$

where $K_\theta = (k_{ij}^{(\theta)})_{i,j=1}^3$, $K_\omega = (k_{ij}^{(\omega)})_{i,j=1}^3$, $K_h = (k_{ij}^{(h)})_{i,j=1}^3$, $k_{ij}^{(\theta)}$, $k_{ij}^{(\omega)}$, $k_{ij}^{(h)}$, $i, j = \overline{1,3}$ are constant values.

The system of equations (5), (21) admits a stationary solution

$$\gamma = -\delta = \pi/2,\ \beta = 0,\ \omega_1 = \omega_2 = \omega_3 + \omega_0 = 0,\ h_1 = h_2 = h_3 = 0. \quad (22)$$

This solution describes the equilibrium position of the spacecraft in the orbital coordinate system, while the orientation of the axes of the system $Ox_1x_2x_3$ corresponds to (7).

The system (4), (5), (21), linearized in the vicinity of solution (22), can be represented as two independent subsystems of the third and sixth order [25]:

$$\dot{\mathbf{x}}_5 = \left(A_5 + B_5 K_5\right)\mathbf{x}_5,\ \mathbf{x}_5 = \left(\omega_3 + \omega_0, \delta + \pi/2, h_3\right)^{\mathrm{T}}, \quad (23)$$

$$A_5 = \begin{pmatrix} 0 & 3\omega_0^2\left(I_1 - I_2\right)/I_3 & 0 \\ -1 & 0 & 0 \\ 0 & 0 & 0 \end{pmatrix},\ B_5 = \left(1/I_3, 0, -1\right)^{\mathrm{T}},\ K_5 = \left(-k_{33}^{(\omega)}, k_{33}^{(\theta)}, k_{33}^{(h)}\right),$$

$$\dot{\mathbf{x}}_6 = \left(A_6 + B_6 K_6\right)\mathbf{x}_6,\ \mathbf{x}_6 = \left(\omega_1, \omega_2, \gamma - \pi/2, \beta, h_1, h_2\right)^{\mathrm{T}}, \quad (24)$$

$$A_6 = \begin{pmatrix} 0 & \omega_0\left(I_3 - I_2\right)/I_1 & -3\omega_0^2\left(I_3 - I_2\right)/I_1 & 0 & 0 & 0 \\ \omega_0\left(I_1 - I_3\right)/I_2 & 0 & 0 & 0 & 0 & 0 \\ 1 & 0 & 0 & -\omega_0 & 0 & 0 \\ 0 & 1 & \omega_0 & 0 & 0 & 0 \\ 0 & 0 & 0 & 0 & 0 & -\omega_0 \\ 0 & 0 & 0 & 0 & \omega_0 & 0 \end{pmatrix},$$

$$B_6 = \begin{pmatrix} 1/I_1 & 0 & 0 & 0 & -1 & 0 \\ 0 & 1/I_2 & 0 & 0 & 0 & -1 \end{pmatrix}^{\mathrm{T}},$$

$$K_6 = \begin{pmatrix} -k_{11}^{(\omega)} & -k_{12}^{(\omega)} & -2k_{11}^{(\theta)} - \omega_0 k_{12}^{(\omega)} & -k_{12}^{(\theta)} + \omega_0 k_{11}^{(\omega)} & k_{11}^{(h)} & k_{12}^{(h)} \\ -k_{21}^{(\omega)} & -k_{22}^{(\omega)} & -2k_{21}^{(\theta)} - \omega_0 k_{22}^{(\omega)} & -k_{22}^{(\theta)} + \omega_0 k_{21}^{(\omega)} & k_{21}^{(h)} & k_{22}^{(h)} \end{pmatrix}.$$

In this case, such a form of the linearized system (23), (24), as well as the structure of matrices K_5, K_6, are due to the fact that the orbital orientation mode of the spacecraft in the vicinity of a gravitationally unstable equilibrium position cannot be implemented without using information about the spacecraft orientation. Here $k_{13}^{(\theta)} = k_{23}^{(\theta)} = k_{31}^{(\theta)} = k_{32}^{(\theta)} = 0$, $k_{13}^{(\omega)} = k_{23}^{(\omega)} = k_{31}^{(\omega)} = k_{32}^{(\omega)} = 0$ and $k_{13}^{(h)} = k_{23}^{(h)} = k_{31}^{(h)} = k_{32}^{(h)} = 0$.

The characteristic polynomial of the third-order system depends on the coefficients $k_{33}^{(\theta)}$, $k_{33}^{(\omega)}$ and $k_{33}^{(\theta)}$, $k_{33}^{(\omega)}$. Let us choose them, as above, so that this polynomial has a triple real root $\lambda_j^{(5)} = -\alpha$, $j = \overline{1,3}$ where $\alpha > 0$ is the degree of stability. We obtain analytical dependencies

$$k_{33}^{(h)} = \frac{\alpha^3 I_3}{3\omega_0^2 (I_1 - I_2)},\ k_{33}^{(\omega)} = I_3 \left(3\alpha - k_{33}^{(h)}\right),\ k_{33}^{(\theta)} = 3\left(I_3 \alpha - \omega_0^2 (I_1 - I_2)\right).$$

For the spacecraft under consideration, we set the value $\alpha = 5.0 \cdot 10^{-3}$ s^{-1}, then $k_{33}^{(h)} = -4.267 \cdot 10^{-2}$ s^{-1}, $k_{33}^{(\omega)} = 628.648$ N·m·s, $k_{33}^{(\theta)} = 0.849$ N·m.

As in section 8, the values of the sixth-order polynomial coefficients will be sought in the form $K_6 = -S^{-1} B_6^{\mathrm{T}} P$, where $P \in \mathbb{R}^{6\times 6}$ is a matrix obtained as a result of numerical solution of the algebraic Riccati matrix equation $PA_6 + A_6^{\mathrm{T}} P - PB_6 S^{-1} B_6^{\mathrm{T}} P + R = 0$. Here $R \in \mathbb{R}^{6\times 6}$ and $S \in \mathbb{R}^{2\times 2}$ are positive definite matrices of weight coefficients, to the selected values of which $R = \mathrm{diag}(1,1,0.01,1,0.01,1)$, $S = \mathrm{diag}(1,1)$ correspond the coefficient values

$$k_{11}^{(\omega)} = 701.26 \text{ N·m·s},\ k_{12}^{(\omega)} = -554.17 \text{ N·m·s},\quad k_{11}^{(\theta)} = 0.19 \text{ N·m},\ k_{12}^{(\theta)} = -0.30 \text{ N·m},$$
$$k_{11}^{(h)} = -0.17 \text{ s}^{-1},\ k_{12}^{(h)} = 0.05 \text{ s}^{-1},$$
$$k_{21}^{(\omega)} = 117.55 \text{ N·m·s},\quad k_{22}^{(\omega)} = 128.15 \text{ N·m·s},\quad k_{21}^{(\theta)} = 0.02 \text{ N·m},\ k_{22}^{(\theta)} = 0.09 \text{ N·m},$$
$$k_{21}^{(h)} = -0.04 \text{ s}^{-1},\ k_{22}^{(h)} = 0.99 \text{ s}^{-1}.$$

The corresponding values of the roots of the sixth-degree characteristic polynomial will be $\lambda_{1,2}^{(6)} = -8.40 \cdot 10^{-5} \pm 1.11 \cdot 10^{-3} i$ s^{-1}, $\lambda_{3,4}^{(6)} = -6.52 \cdot 10^{-4} \pm 1.47 \cdot 10^{-4} i$ s^{-1},
$$\lambda_5^{(6)} = -9.83 \cdot 10^{-2} \text{ s}^{-1},\ \lambda_6^{(6)} = -1.00 \text{ s}^{-1}.$$

The degree of stability of the sixth-order polynomial $\alpha = 8.40 \cdot 10^{-5}$ s^{-1}. Thus, the control law (21) with the specified parameter values $k_{ij}^{(\theta)}$ $k_{ij}^{(\omega)}$, $k_{ij}^{(h)}$, $i, j = \overline{1,3}$ ensures the asymptotic stability of the system (3), (4) in the neighborhood of the stationary solution (22).

Let us show that for the found coefficient values $k_{ij}^{(\theta)}$ $k_{ij}^{(\omega)}$, $k_{ij}^{(h)}$, $i, j = \overline{1,3}$ the law of change of the gyrosystem control moment (21) indeed provides the spacecraft orientation close to the gravitationally unstable equilibrium position. For this purpose, we will calculate the solutions of the system (3), (4), (21) with initial conditions $\beta(0) = 0$, $\gamma(0) = -\delta(0) = \pi/2$, $\omega_1(0) = \omega_2(0) = \omega_3(0) + \omega_0 = 0.01$ °/s, $h_1(0) = h_2(0) = h_3(0) = 0$ over a time interval of 8 days. In Fig. 8, 9 show graphs of time dependency of angles γ, δ, β, components h_i, $i = \overline{1,3}$ and the modulus of the gyrostatic moment $|\mathbf{H}|$. The graphs do not show the initial section with a duration of 1 day, containing the transient process, which is caused by errors in setting the initial angular velocity. The calculation results show that the control law (21) provides stable orbital orientation of the spacecraft, and the gyrostatic moment remains limited. In the steady state, the amplitudes of the angular velocity components' oscillations are limited to the following values:

$$|\omega_1| < 1.5 \cdot 10^{-4} \text{ °/s}, |\omega_2| < 1 \cdot 10^{-4} \text{ °/s}, |\omega_3| < 2 \cdot 10^{-3} \text{ °/s}.$$

Fig. 8. Spacecraft orientation angles when using control law (21)

Fig. 9. Components and modulus of the spacecraft gyrostatic moment vector when using control law (21)

In Fig. 8, the gradual decrease in the amplitude of oscillations of angles γ, β is caused by the residual influence of the transient process occurring during the first day of spacecraft flight. Here, the steady-state oscillations of values γ, δ, β, ω_i, h_i, $i = \overline{1,3}$ and $|\mathbf{H}|$ also occur with a dominant frequency equal to the orbital frequency ω_0.

CONCLUSION

The paper shows that using gyroscopic actuators of the spacecraft rotational motion control system, it is possible to implement a mode of long-term orbital orientation of the spacecraft both in the vicinity of the gravitationally stable and unstable equilibrium position.

The corresponding control laws for the intrinsic kinetic moment of the gyrosystem are provided. As the main mode for implementing orbital orientation of the spacecraft in the vicinity of the stable equilibrium position, the gyrodamping mode is considered, for which the results of numerical modeling of microaccelerations occurring on board the spacecraft, as well as their amplitude spectra, are presented. It is shown that this mode can be used when conducting space experiments during long time intervals.

Additionally, two more variants of the gyrosystem control law have been considered, which provide orbital orientation of the spacecraft in the vicinity of stable and unstable equilibrium

positions. For all considered variants, a methodology for selecting control law coefficients that ensure asymptotic stability of the spacecraft's rotational motion is proposed.

All gyrosystem control laws proposed in this work allow not only to provide a specified orientation of the spacecraft but also to limit the accumulation of gyrostatic moment.

The results obtained in this work can be used in the preliminary design of spacecraft attitude control systems built on the basis of various types of gyroscopic control devices.

REFERENCES

1. *Sazonov V.V., Chebukov S.Yu., Abrashkin V.I., et al.* Analysis of low-frequency microaccelerations aboard the satellite *Foton-11* // Cosmic Research. 2001. Vol. 39. No. 4. P. 419-435.
2. *Boizielink T., Van Bavinkhov K., Sazonov V.V. et al.* Analysis of the low-frequency component in microacceleration measurements performed on the satellite *Foton M-2* // Cosmic Research. 2008. Vol. 46. No. 5. P. 463-483.
3. *Ignatov A.I., Sazonov V.V.* Implementation of satellite rotational motion modes with low level of microaccelerations by electromechanical actuators // Cosmic Research. 2012. Vol. 50. No. 5. P. 380-393.
4. *Sarychev V.A., Sazonov V.V.* Influence of aerodynamic moment on the gravity-gradient orientation mode of the orbital complex *Salyut-6* Soyuz *Union* // Cosmic Research. 1985. Vol. 23. No. 1. P. 63-67.
5. *Sazonov V.V.* On one mechanism of stability loss in the satellite gravity-gradient orientation mode // Cosmic Research. 1989. Vol. 27. No. 6. P. 836-841.
6. *Sarychev V.A.* Issues of artificial satellite orientation // Results of Science and Technology. Ser. Space Research. Vol. 11. Moscow: VINITI, 1978. 223 p.
7. *Sazonov V.V.* Gravity-gradient orientation of artificial satellites with control moment gyroscopes // Cosmic Research. 1988. Vol. 26. No. 2. P. 315-318.
8. *Ignatov A.I., Sazonov V.V.* Implementation of the Earth Satellite Orbital Orientation Mode Without Kinetic Moment Accumulation of the Gyro System // Proceedings of the Russian Academy of Sciences. Theory and Control Systems. 2020. No. 1. P. 129–142.
9. *Zubov N.E., Mikrin E.A., Misrikhanov M.Sh. et al.* Stabilization of Spacecraft Orbital Orientation with Simultaneous Unloading of the Kinetic Moment of Inertial Actuators // Proceedings of the Russian Academy of Sciences. Theory and Control Systems. 2015. No. 4. P. 124–131.
10. *Mashtakov Y., Tkachev S., Ovchinnikov M.* Use of External Torques for Desaturation of Reaction Wheels // Guidance, Control and Dynamics. 2018. V. 41. Iss. 8. P. 1663–1674.
11. *Sazonov V.V., Komarov M.M., Polezhaev V.I. et al.* Microaccelerations on the Orbital Station *Mir* and Operational Analysis of the Gravitational Sensitivity of Convective Heat and Mass Transfer Processes // Space Research. 1999. V. 37. No. 1. P. 86–101.
12. *Ignatov A.I., Sazonov V.V.* Estimation of Residual Microaccelerations Onboard a Satellite in the Mode of Single-Axis Solar Orientation // Space Research. 2013. V. 51. No. 5. P. 380–388.
13. *Ignatov A.I.* Estimation of Low-Frequency Microaccelerations Onboard an Earth Artificial Satellite in Solar Orientation Mode // Space Research. 2022. V. 60. No. 5. P. 43–56.
14. *Ignatov A.I., Ivanov G.A., Kolomiets E.S. et al.* Implementation of Spacecraft Solar Orientation Mode Using a System of Reaction Wheels // Space Research. 2023. V. 61. No. 2. P. 143–156.

15. *Beletsky V.V.* Motion of an Artificial Satellite About its Center of Mass. Moscow: Nauka, 1965. 415 p.
16. *Beletsky V.V., Yanshin A.M.* Influence of Aerodynamic Forces on the Rotational Motion of Artificial Satellites. Kiev: Naukova Dumka, 1984. 187 p.
17. *Barbashin E.A.* Lyapunov Functions. Moscow: Nauka, 1970. 240 p.
18. *Sarychev V.A.* Stability Conditions for a Satellite Gravity-Gradient Stabilization System with Gyro Damping // Astronautica Acta. 1969. V. 14. Iss. 4. P. 299–301.
19. *Rumyantsev V.V.* On the stability of stationary satellite motions // Ser. Mathematical methods in spacecraft dynamics. Issue 4. Moscow: Computing Center of the USSR Academy of Sciences, 1967. 141 p.
20. *Ignatov A.I.* Selection of geometric parameters for the placement of a system of flywheel engines for controlling the rotational motion of a spacecraft // Izv. RAS. Control Sciences. 2022. No. 1. P. 124–144.
21. *Zemskov V.S., Raukhman M.R., Shalimov V.P* . Gravitational sensitivity of solution-melts during crystallization of two-phase InSb-InBi alloys in space conditions // Space Research. 2001. Vol. 39. No. 4. P. 384–389.
22. *Terebizh V.Yu.* Analysis of time series in astrophysics. Moscow: Nauka, 1992. 392 p.
23. *Ignatov A.I., Kolomiets E.S., Martynenkova E.V.* Implementation of the gravitational orientation mode of a spacecraft without accumulating the kinetic moment of the gyro system // Proceedings of the XIII All-Russian Congress on Theoretical and Applied Mechanics. Saint Petersburg, Russia. 2023. Vol. 1. P. 593–595.
24. *Polyak B.T., Khlebnikov M.V., Rapoport L.B.* Mathematical theory of automatic control. Moscow: LENAND, 2019. 504 p.
25. *Ignatov A.I., Kolomiets E.S., Martynenkova E.V.* Maintaining the orbital orientation mode of a spacecraft in the vicinity of a gravitationally unstable equilibrium position // Proceedings of the XIII All-Russian Congress on Theoretical and Applied Mechanics. Saint Petersburg, Russia. 2023. Vol. 1. P. 591–592.

Figure captions

Fig. 1. General shape of the spacecraft and position of the body-fixed coordinate system

Fig. 2. Spacecraft orientation angles when using control law (12)

Fig. 3. Components and magnitude of spacecraft gyrostatic moment vector when using control law (12)

Fig. 4. Components and magnitude of spacecraft microacceleration vector

Fig. 5. Amplitude spectra of vector magnitudes $\mathbf{b}_a$, $\mathbf{b}_g$ and $\mathbf{b}$

Fig. 6. Spacecraft orientation angles when using control law (17)

Fig. 7. Components and magnitude of spacecraft gyrostatic moment vector when using control law (17)

Fig. 8. Spacecraft orientation angles when using control law (21)

Fig. 9. Components and magnitude of spacecraft gyrostatic moment vector when using control law (21)

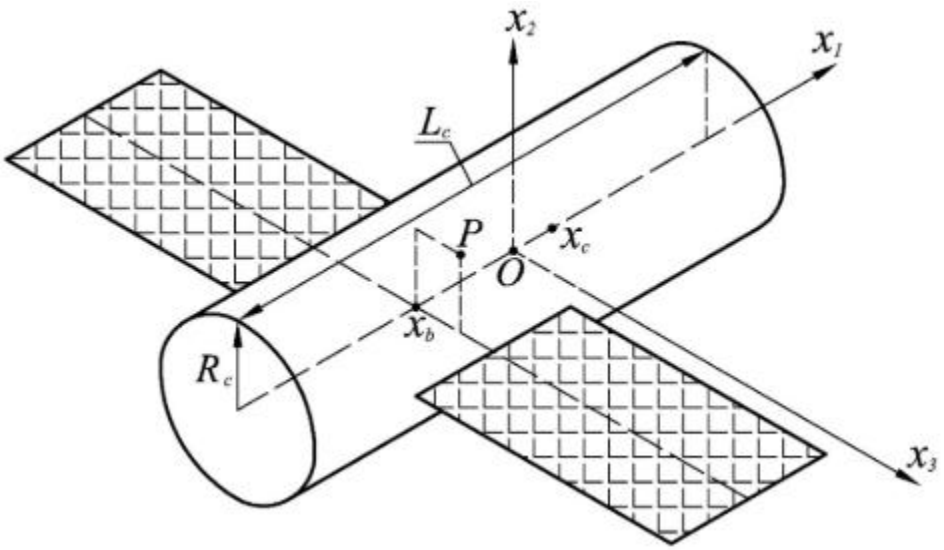

Fig. 1. General shape of the spacecraft and position of the body-fixed coordinate system

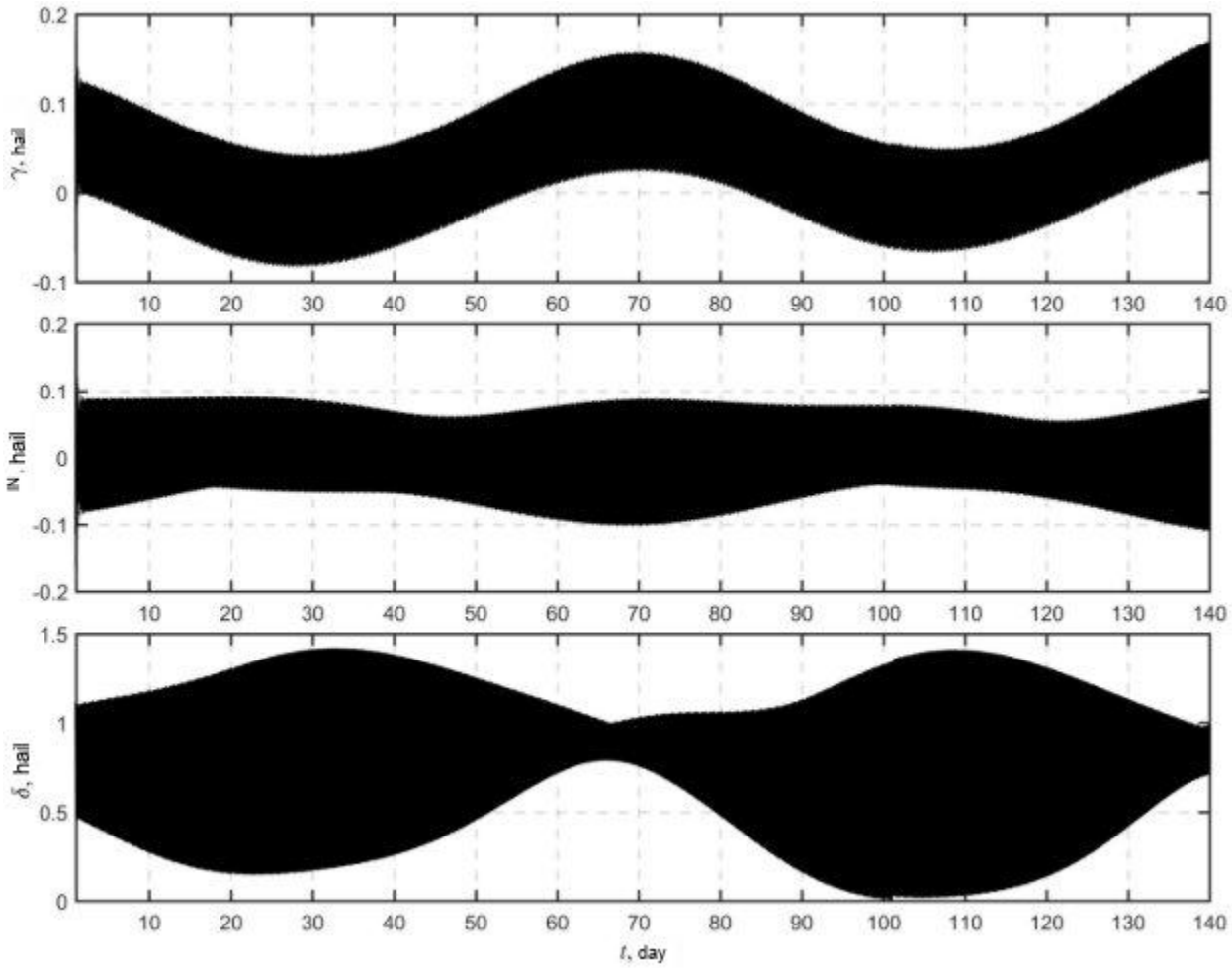

Fig. 2. Spacecraft orientation angles when using control law (12)

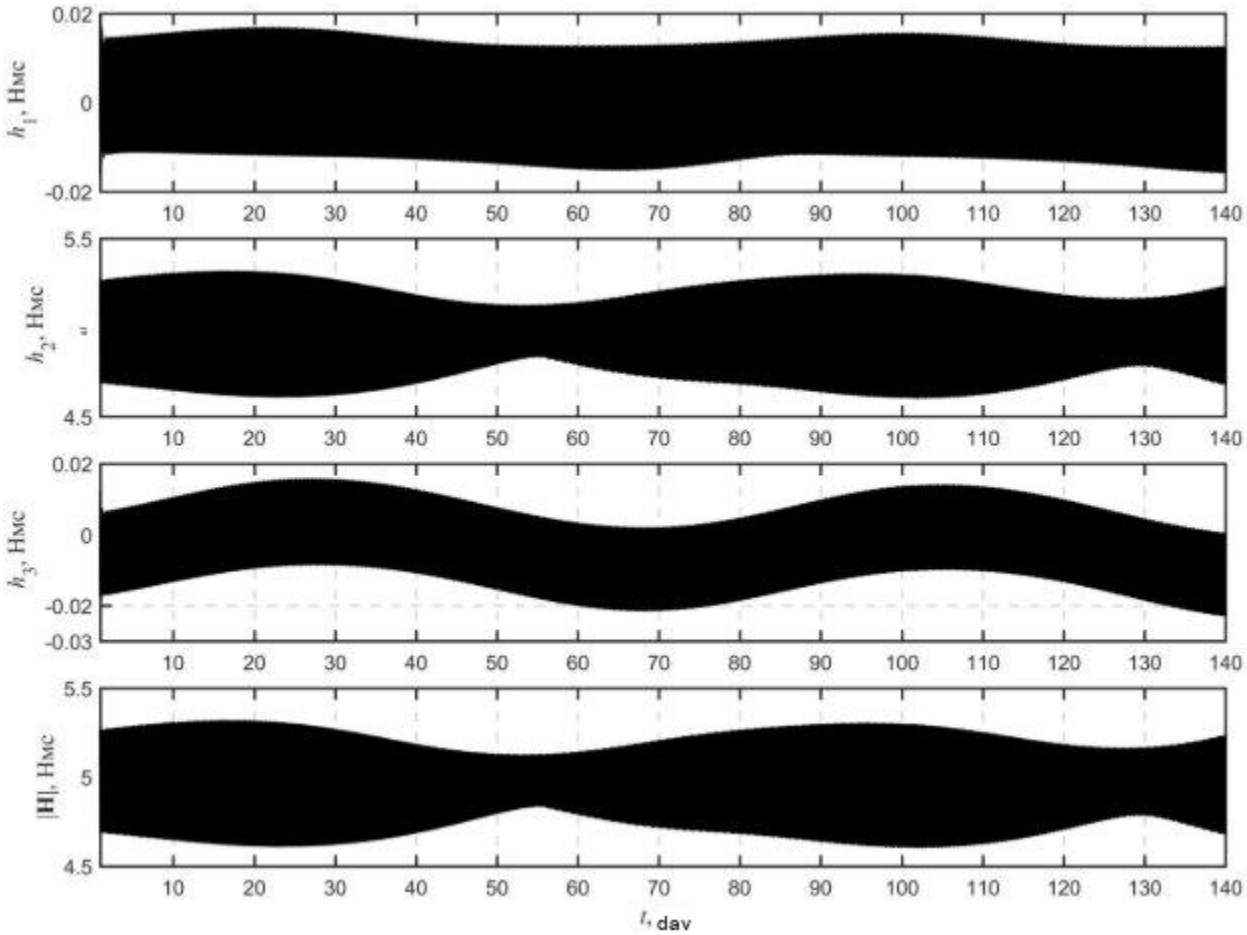

Fig. 3. Components and magnitude of spacecraft gyrostatic moment vector when using control law (12)

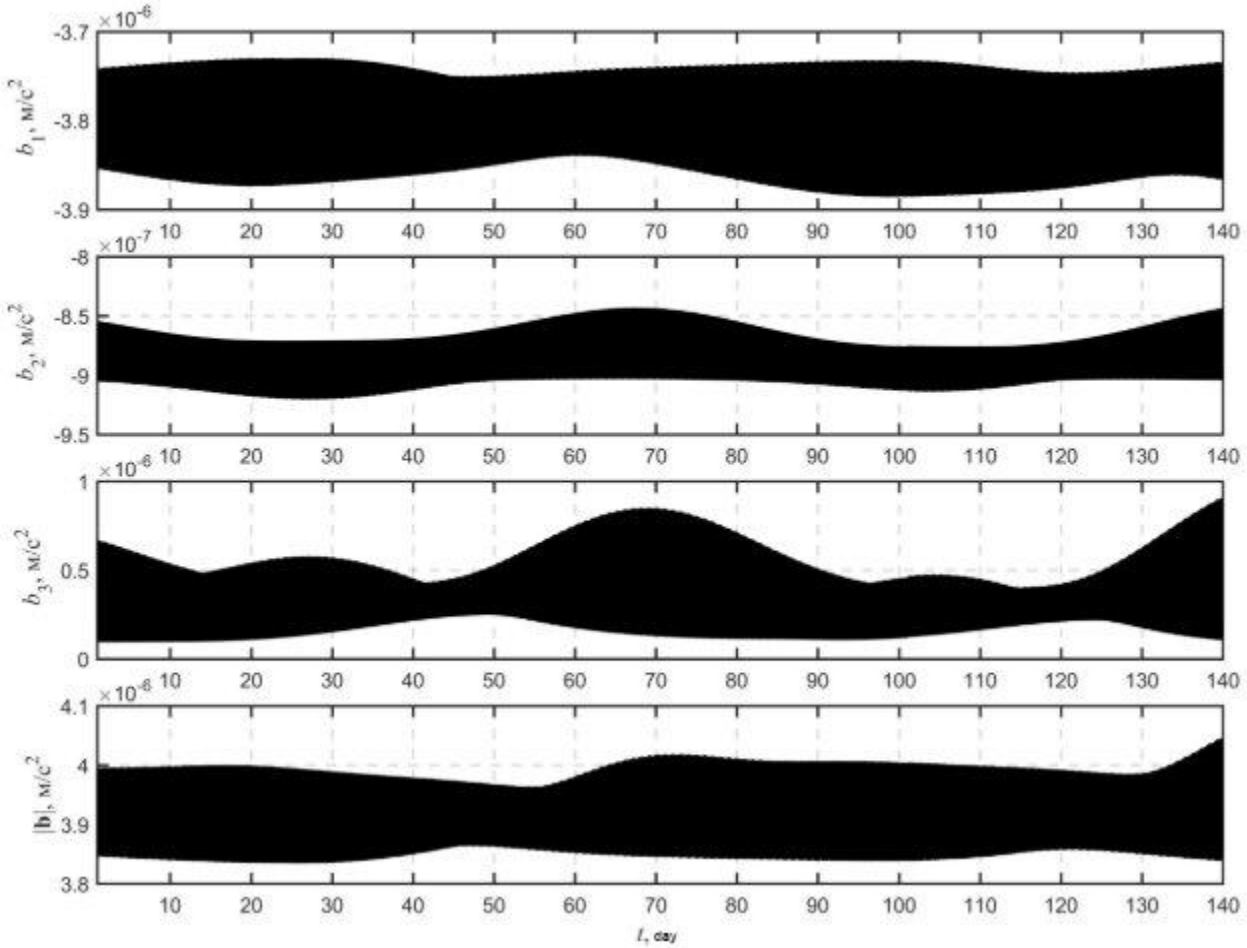

Fig. 4. Components and magnitude of spacecraft microacceleration vector

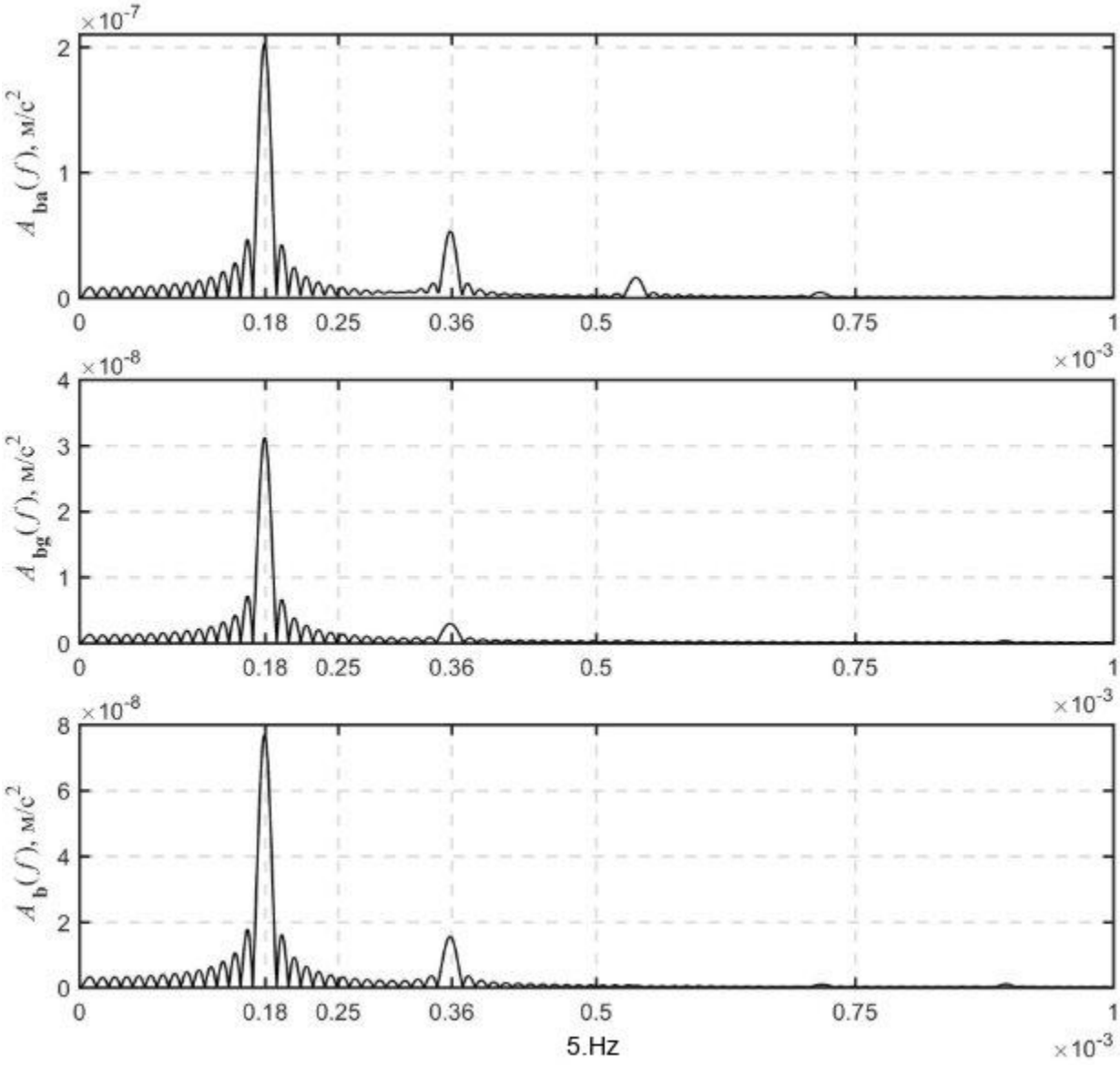

Fig. 5. Amplitude spectra of vector magnitudes $\mathbf{b}_a$, $\mathbf{b}_g$ and $\mathbf{b}$

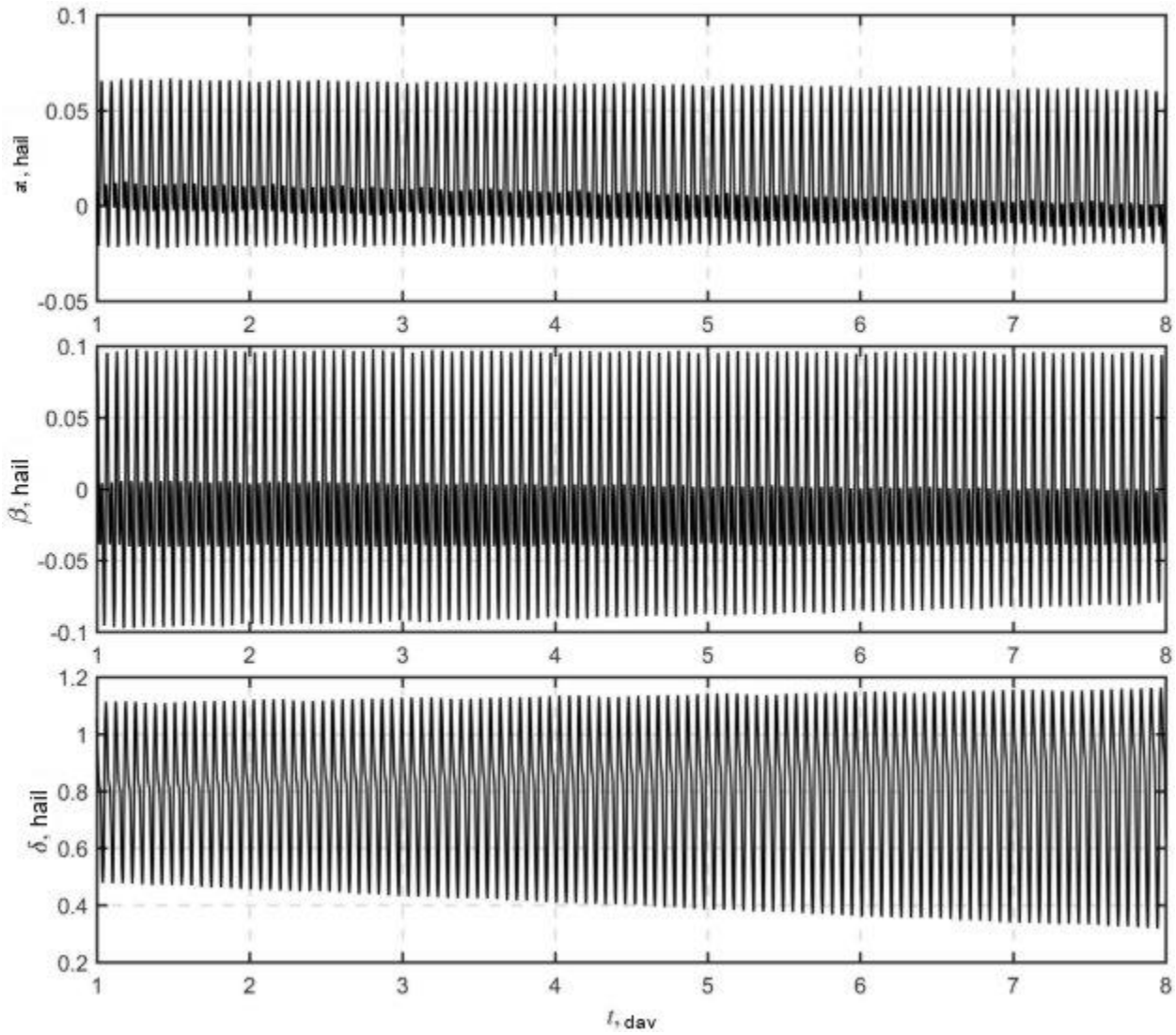

Fig. 6. Spacecraft orientation angles when using control law (17)

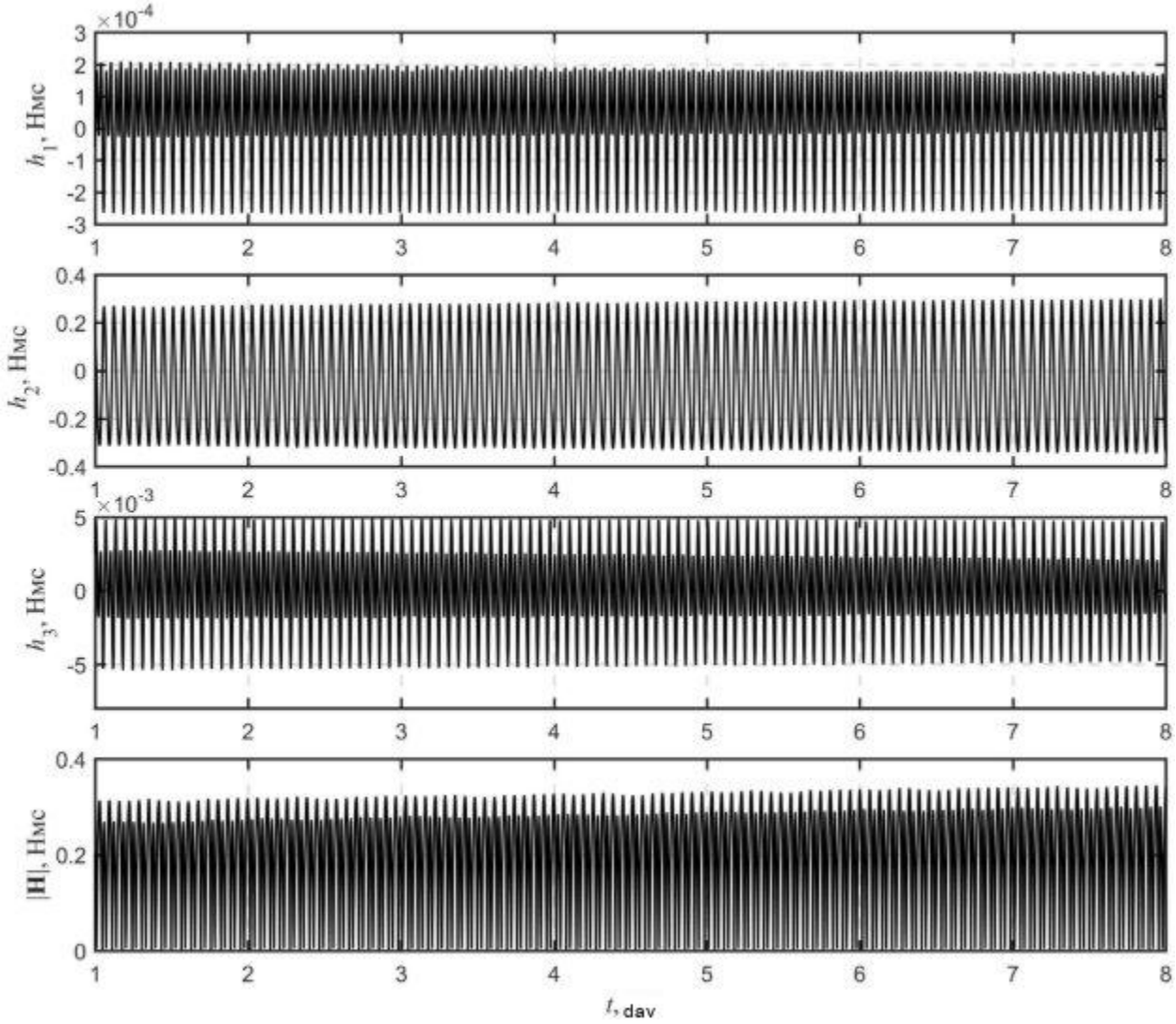

Fig. 7. Components and magnitude of spacecraft gyrostatic moment vector when using control law (17)

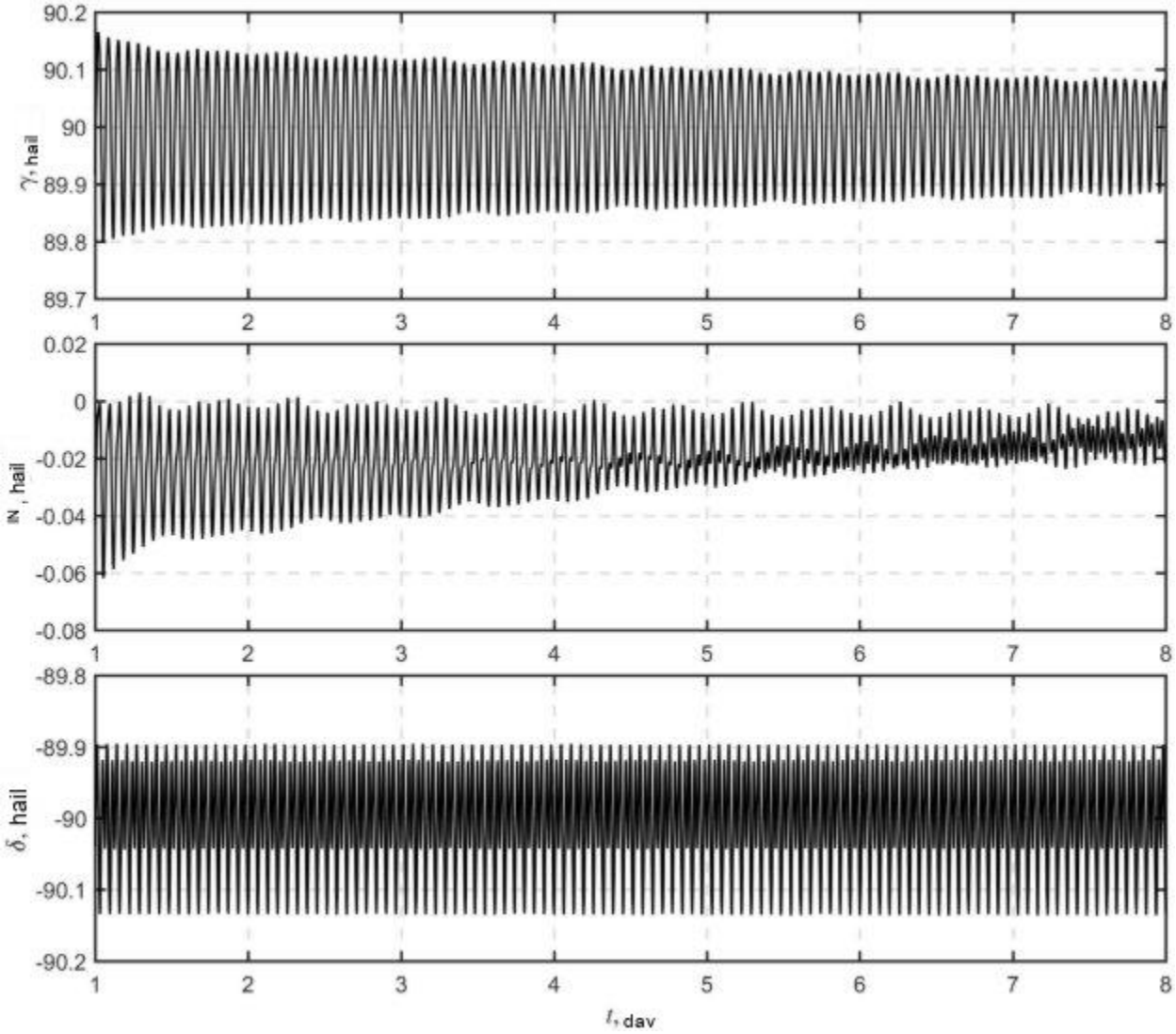

Fig. 8. Spacecraft orientation angles when using control law (21)

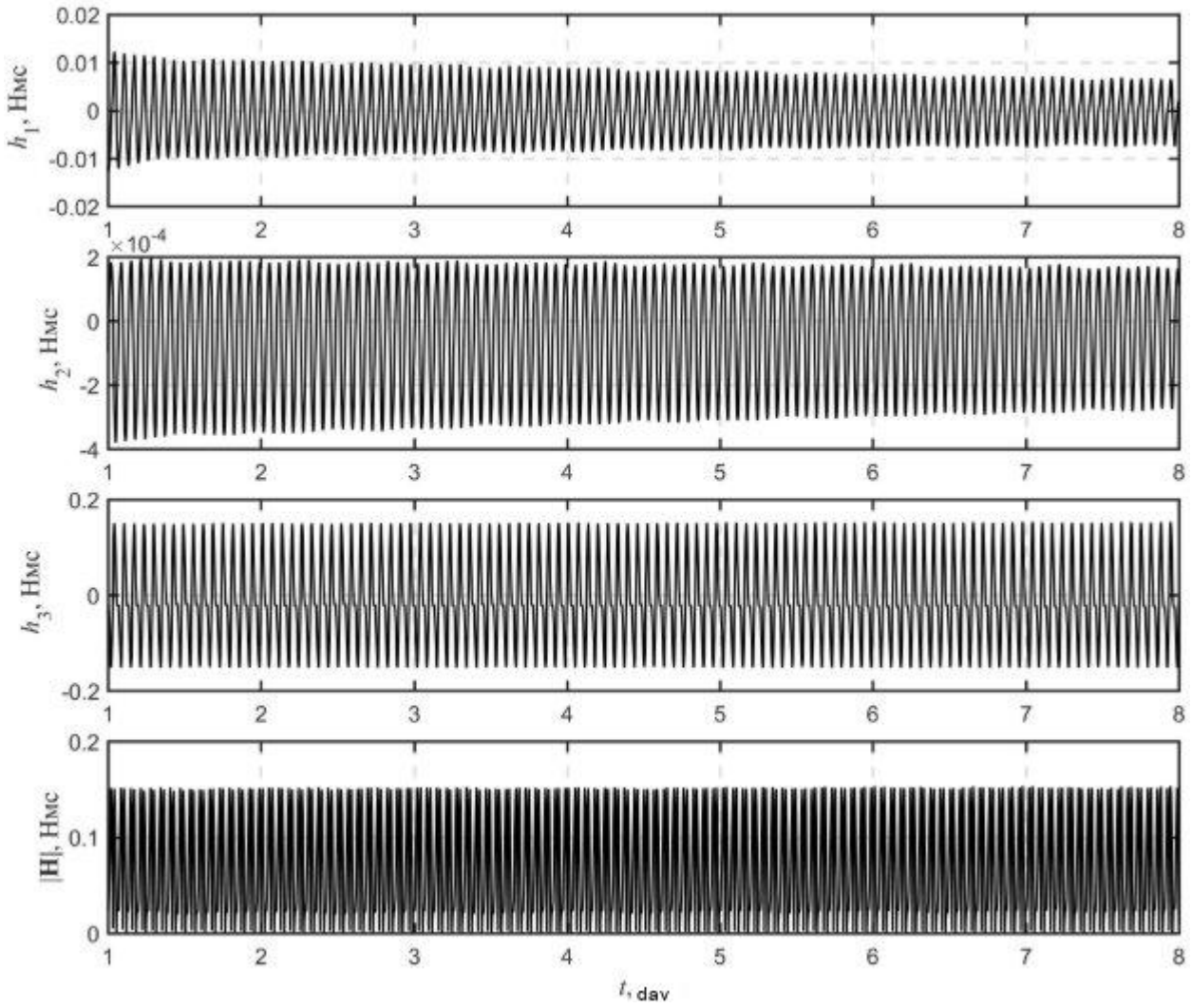

Fig. 9. Components and magnitude of spacecraft gyrostatic moment vector when using control law (21)